Journal of Solid State Chemistry **147,** 140–145 (1999)
Article ID jssc.1999.8197, available online at http://www.idealibrary.com on IDEAL®

Nonstoichiometric Rare-Earth Copper Arsenides *RE*Cu$_{1+x}$As$_2$ (*RE* = La, Ce, Pr)

Meitian Wang, Robert McDonald,[1] and Arthur Mar[2]

Department of Chemistry, University of Alberta, Edmonton, Alberta, Canada T6G 2G2
E-mail: amar@gpu.srv.ualberta.ca

Received September 22, 1998; in revised form January 20, 1999; accepted February 2, 1999

IN MEMORY OF JEAN ROUXEL

Single crystals of the ternary rare-earth copper arsenides *RE*Cu$_{1+x}$As$_2$ (*RE* = La, Ce, Pr) have been prepared by reactions of the elements in the presence of I$_2$, and their structures have been determined by X-ray diffraction. They crystallize in tetragonal space groups, with the La member in *I*4/*mmm* (LaCu$_{1.23(1)}$As$_2$, $a = 4.0901(4)$ Å, $c = 20.243(3)$ Å, $Z = 4$) and the Ce and Pr members in *P*4/*nmm* (CeCu$_{1.10(1)}$As$_2$, $a = 4.0265(4)$ Å, $c = 10.071(2)$ Å, PrCu$_{1.09(1)}$As$_2$, $a = 4.0086(2)$ Å, $c = 10.0496(9)$ Å; $Z = 2$ for both). LaCu$_{1.23(1)}$As$_2$ represents a stuffed variant of the SrZnBi$_2$ structure type, while CeCu$_{1.10(1)}$As$_2$ and PrCu$_{1.09(1)}$As$_2$ are stuffed variants of the HfCuSi$_2$ structure type. The nonstoichiometry of these compounds arises from partial occupation of a square pyramidal site by Cu. The structural chemistry of these ternary arsenides is thus more complicated than previously assumed. Magnetic susceptibility measurements indicate diamagnetism for LaCu$_{1.23(1)}$As$_2$, paramagnetism for CeCu$_{1.10(1)}$As$_2$, and antiferromagnetism ($T_N \approx 4$K) for PrCu$_{1.09(1)}$As$_2$. © 1999 Academic Press

Key Words: **rare-earth; arsenide; crystal structure; synthesis.**

INTRODUCTION

Our continued interest in the preparation of new ternary rare-earth transition-metal pnictides derives from the wide array of physical properties they exhibit. Investigation of these ternary pnictides to date has been largely restricted to the late transition metals, and the arsenides are no exception, with an enormous number of ternary rare-earth nickel arsenides known, for instance (1). In the *RE*/Cu/As system (*RE* = rare-earth), the compounds EuCuAs (Ni$_2$In-type) (2), EuCu$_{2-x}$As$_2$ (ThCr$_2$Si$_2$-type) (3), and *RE*CuAs$_2$ (*RE* = La–Nd, Sm, Gd–Lu) (HfCuSi$_2$-type) (4) have been reported previously. The isotypy of *RE*CuAs$_2$ to HfCuSi$_2$ (5) was assumed on the basis of evidence from powder X-ray diffraction data (4). We report here the single crystal structures of the nonstoichiometric phases, *RE*Cu$_{1+x}$As$_2$ (*RE* = La, Ce, Pr), prepared under different synthetic conditions and demonstrate that the presence of excess Cu can lead to the formation of a stuffed variant of the ideal, stoichiometric *RE*CuAs$_2$ structure. The magnetic susceptibilities of these compounds are also presented.

EXPERIMENTAL

Synthesis

Reactions of powders of the elements (>99.9% purity, obtained from Alfa-Aesar or Cerac) were generally carried out on a ~ 0.25-g scale in evacuated fused-silica tubes (8-cm length; 10-mm i.d.). Elemental compositions (EDX analysis) of selected crystals were determined on a JEOL JSM-6301FXV field-emission scanning electron microscope. X-ray powder patterns were obtained on an Enraf-Nonius FR552 Guinier camera (Cu$K\alpha_1$ radiation; Si standard).

A ternary phase containing excess copper, LaCu$_{1+x}$As$_2$, was first identified in a reaction of La, Hf, Cu, and As in a 1:2:4:4 ratio, heated at 1000°C for 4 days. Among the products, consisting largely of a mixture of known binary phases, were square plate- or block-shaped crystals exhibiting a doubled *c* axis relative to the reported parameters for LaCuAs$_2$ (4) and an elemental composition consistent with the presence of excess copper (mol%: La, 24(1); Cu, 30(1); As, 46(1)). A series of reactions was then performed, La + $(1+x)$Cu + 2As ($x = 0$, 0.1, 0.2, 0.3, 0.4, 0.5), at 1000°C for 4 days. The resulting products were microcrystalline powders that consisted essentially of the nonstoichiometric phase identified above, designated as LaCu$_{1+x}$As$_2$, for $x \le 0.3$. Beyond $x = 0.3$, impurities of binary arsenides appear. Single crystals could be obtained via a more rational route by reaction of the elements in a two-zone furnace (900/950°C) with the addition of I$_2$

---

[1] Faculty Service Officer, Structure Determination Laboratory.

[2] Author to whom correspondence should be addressed. E-mail: amar@gpu.srv.ualberta.ca

0022-4596/99 $30.00

TABLE 1
Cell Parameters for $RE\mathrm{Cu}_{1+x}\mathrm{As}_2$ (RE=La, Ce, Pr)

Compound	a (Å)	c (Å)	V (Å^3)
$\mathrm{LaCu}_{1.23(1)}\mathrm{As}_2$	4.0984(9)	20.280(8)	340.6(2)
$\mathrm{CeCu}_{1.10(1)}\mathrm{As}_2$	4.030(1)	10.089(4)	163.8(1)
$\mathrm{PrCu}_{1.09(1)}\mathrm{As}_2$	4.011(2)	10.055(4)	161.8(1)

($\sim$10 mg) as a mineralizing agent. Well-formed silver square plates or blocks were found at the hot end of the silica tube. EDX analyses of these crystals invariably revealed a composition with excess copper, $RE\mathrm{Cu}_{1+x}\mathrm{As}_2$, independent of the amount of Cu loaded. The crystals used for the structure determinations resulted from the following reactions and possessed the indicated elemental compositions: $\mathrm{LaCu}_{1.23(1)}\mathrm{As}_2$, La + 1.1Cu + 2As, 23(1)% La, 27(1)% Cu, 50(1)% As; $\mathrm{CeCu}_{1.10(1)}\mathrm{As}_2$, Ce + 0.7Cu + 2As, 23(1)% Ce, 25(1)% Cu, 52(1)% As; $\mathrm{PrCu}_{1.09(1)}\mathrm{As}_2$, Pr + 1.5Cu + 2As, 24(1)% Pr, 25(1)% Cu, 51(1)% As. Powder X-ray diffraction data were obtained on crushed crystals from these reactions, and the cell parameters that were refined with the use of the program POLSQ (6) are listed in Table 1.

Structure Determination

Two X-ray structure determinations were performed for $\mathrm{LaCu}_{1+x}\mathrm{As}_2$, the first on the crystal from the original reaction, which leads to a refined formula of $\mathrm{LaCu}_{1.27(1)}\mathrm{As}_2$, and the second on a crystal obtained from the rational reaction, which leads to a refined formula of $\mathrm{LaCu}_{1.23(1)}\mathrm{As}_2$. These formulas are in good agreement with their respective EDX compositions indicated above. It suffices to report only the latter determination, as the results are similar. Weissenberg photography clearly reveals a doubled c axis and body centering systematic absences (hkl: $h + k + l = 2n + 1$) consistent with several possible tetragonal space groups, the centrosymmetric space group $I4/mmm$ being chosen on the basis of the successful refinement and the structural relationship to similar compounds. For $\mathrm{CeCu}_{1.10(1)}\mathrm{As}_2$ and $\mathrm{PrCu}_{1.09(1)}\mathrm{As}_2$, in contrast, the Weissenberg photographs confirm the presence of an undoubled c axis, a primitive unit cell, and systematic absences ($0kl$: $k + l = 2n + 1$) consistent with the tetragonal space group $P4/nmm$ previously found for $RE\mathrm{CuAs}_2$ (4), but with slightly larger cell parameters. Final cell parameters were determined from least-squares analyses of 24 reflections centered on an Enraf-Nonius CAD-4 diffractometer in the range $12° \leq 2\theta(\mathrm{Mo}K\alpha) \leq 20°$ for $\mathrm{LaCu}_{1.23(1)}\mathrm{As}_2$, $20° \leq 2\theta(\mathrm{Mo}K\alpha) \leq 43°$ for $\mathrm{CeCu}_{1.10(1)}\mathrm{As}_2$, and $25° \leq 2\theta(\mathrm{Mo}K\alpha) \leq 42°$ for $\mathrm{PrCu}_{1.09(1)}\mathrm{As}_2$. Intensity data were collected at room temperature with the θ–2θ scan technique in the range $4° \leq 2\theta(\mathrm{Mo}K\alpha) \leq 70°$. Calculations were carried out with the use of the SHELXTL (Version 5.1) package (7). Conventional atomic scattering factors and anomalous dispersion corrections were used (8). Intensity data were processed, and face-indexed absorption corrections were applied in XPREP (7). Initial atomic positions were found by direct methods, and refinements were performed by least-squares methods.

Refinements of the $\mathrm{LaCu}_{1.23(1)}\mathrm{As}_2$ structure to this stage were on a model identical to the atomic arrangement of the UCuP_2 (SrZnBi_2-type) structure (9); similarly, the model in $\mathrm{CeCu}_{1.10(1)}\mathrm{As}_2$ or $\mathrm{PrCu}_{1.09(1)}\mathrm{As}_2$ was identical to that of the reported $RE\mathrm{CuAs}_2$ (HfCuSi_2-type) structure (4). In each case, however, the difference Fourier maps reveal pronounced residual electron density in the vicinity of a square pyramidal site that is vacant in the parent structures. Given the consistently higher percentage of Cu observed in the EDX analyses relative to the ideal formula $RE\mathrm{CuAs}_2$, additional Cu atoms were assigned to this site and allowed to refine isotropically at partial occupancy. These refinements result in significant improvements in the agreement factors (e.g., R/R_w decrease from 0.037/0.110 to 0.021/0.061 for $\mathrm{CeCu}_{1.10(1)}\mathrm{As}_2$ on the absorption-corrected data). Another possibility is that this site may be fully occupied by oxygen atoms, since the distance to the five surrounding As atoms ($\sim$2.4 Å) is also reasonable for an As–O bond. However, this model can be ruled out on the basis of windowless EDX measurements showing no evidence for oxygen, and more convincingly, chemical arguments discussed in more detail below. Refinements were attempted in lower symmetry space groups, specifically those that remove the symmetry plane normal to c (e.g., $I\bar{4}$), but these did not lead to any models in which the partially occupied Cu site becomes ordered, nor did consideration of twinning possibilities prove fruitful.

The atomic positions were standardized in STRUCTURE TIDY (10), but we have opted to override the atom numbering that the program suggests for $\mathrm{LaCu}_{1.23(1)}\mathrm{As}_2$ in order to draw structural comparisons with greater ease. The final cycle of least-squares refinement on F_0^2 included anisotropic displacement parameters for all atoms except the partially occupied Cu site, for which simultaneous refinement of occupancy and anisotropic displacement parameters is not recommended because of their strong correlation. Crystal data and further details of the structure determination are given in Table 2. Final values of the positional and displacement parameters are given in Table 3. Anisotropic displacement parameters are given in Table S1, and final structure amplitudes are in Tables S2–S4 (11).

Magnetic Susceptibility

The magnetic data were collected on a Quantum Design SQUID magnetometer. Powder samples ($\sim$20 mg) were

TABLE 2
Crystallographic Data for $RE\mathrm{Cu}_{1+x}\mathrm{As}_2$ (RE=La, Ce, Pr)

Formula	$\mathrm{LaCu}_{1.23(1)}\mathrm{As}_2$	$\mathrm{CeCu}_{1.10(1)}\mathrm{As}_2$	$\mathrm{PrCu}_{1.09(1)}\mathrm{As}_2$
Formula mass (amu)	367.06	359.85	360.49
Space group	$I4/mmm$ (No. 139)	$P4/nmm$ (No. 129)	$P4/nmm$ (No. 129)
a (Å)^a	4.0901(4)	4.0265(4)	4.0086(2)
c (Å)^a	20.243(3)	10.071(2)	10.0496(9)
V(Å^3)	338.64(7)	163.28(3)	161.49(2)
Z	4	2	2
ρ_{calc} (g cm^{-3})	7.200	7.319	7.414
Crystal dimensions (mm)	$0.30 \times 0.29 \times 0.08$	$0.16 \times 0.13 \times 0.10$	$0.14 \times 0.09 \times 0.09$
Radiation	Graphite monochromated Mo$K\alpha$, $\lambda = 0.71073$ Å		
μ(Mo$K\alpha$) (cm^{-1})	392	407	421
Transmission factors	0.010–0.094	0.016–0.101	0.021–0.114
2θ limits	$4° \leq 2\theta(\mathrm{Mo}K\alpha) \leq 70°$	$4° \leq 2\theta(\mathrm{Mo}K\alpha) \leq 70°$	$4° \leq 2\theta(\mathrm{Mo}K\alpha) \leq 70°$
Data collected	$-6 \leq h \leq 6,\ -6 \leq k \leq 6,$ $-32 \leq l \leq 32$	$-6 \leq h \leq 6,\ -6 \leq k \leq 6,$ $-16 \leq l \leq 16$	$-6 \leq h \leq 6,\ -6 \leq k \leq 6,$ $-16 \leq l \leq 16$
No. of data collected	2990	2844	2801
No. of unique data, including $F_o^2 < 0$	272 ($R_{\mathrm{int}} = 0.116$)	260 ($R_{\mathrm{int}} = 0.112$)	258 ($R_{\mathrm{int}} = 0.149$)
No. of unique data, with $F_o^2 > 2\sigma(F_o^2)$	264	248	243
No. of variables^b	16	15	15
$R(F)$ for $F_o^2 > 2\sigma(F_o^2)^c$	0.034	0.020	0.039
$R_w(F_o^2)^d$	0.073	0.050	0.089
Goodness of fit	1.16	1.11	1.21
$(\Delta\rho)_{\max}$, $(\Delta\rho)_{\min}$ (e$^-$Å^{-3})	1.7, -2.4	1.2, -1.5	3.2, -6.3

^{a}Obtained from a refinement constrained so that $a = b$ and $\alpha = \beta = \gamma = 90°$.

^{b}Including an extinction coefficient.

^{c}$R(F) = \sum \| F_o| - |F_c \| / \sum |F_o|$.

^{d}$R_w(F_o^2) = [\sum[w(F_o^2 - F_c^2)]/\sum wF_o^4]^{1/2}$; $w^{-1} = [\sigma^2(F_o^2) + (Ap)^2 + Bp)]$, where $p = [\max(F_o^2, 0) + 2F_c^2]/3$, $A = 0.0310$, 0, and 0.0457, and $B = 4.3152$, 0.3448, and 0.4457 for $\mathrm{LaCu}_{1.23(1)}\mathrm{As}_2$, $\mathrm{CeCu}_{1.10(1)}\mathrm{As}_2$, and $\mathrm{PrCu}_{1.09(1)}\mathrm{As}_2$, respectively.

placed in gelatin capsules. Zero field cooled data were obtained at applied fields ranging from 0.1 to 3 T at temperatures between 5 K (2 K for $\mathrm{PrCu}_{1.09(1)}\mathrm{As}_2$) and 300 K.

RESULTS AND DISCUSSION

The structures of $RE\mathrm{Cu}_{1+x}\mathrm{As}_2$ (RE = La, Ce, Pr) are shown in Fig. 1, and interatomic distances are listed in Table 4. The structures consist of anionic layers of edge-sharing CuAs_4 tetrahedra segregated from square nets of As atoms by the intervening RE cations. $\mathrm{LaCu}_{1.23(1)}\mathrm{As}_2$ is related to $\mathrm{CeCu}_{1.10(1)}\mathrm{As}_2$ (or $\mathrm{PrCu}_{1.09(1)}\mathrm{As}_2$) by doubling of the c axis, which results from an alternation in the relative orientation of the CuAs_4 tetrahedra along this direction. The CuAs_4 tetrahedra are fairly regular, with four equivalent Cu(1)–As(2) bonds at angles close to ideal ($\mathrm{LaCu}_{1.23(1)}\mathrm{As}_2$, 2.5196(6) Å, 108.52(4)–109.95(2)°; $\mathrm{CeCu}_{1.10(1)}\mathrm{As}_2$, 2.5136(5) Å, 106.44(3)–111.01(1)°; $\mathrm{PrCu}_{1.09(1)}\mathrm{As}_2$, 2.5118(6) Å, 105.86(4)–111.30(2)°). These Cu(1) atoms are also arranged in a square net, but the Cu(1)–Cu(1) distances (2.8–2.9 Å) are probably too long to be considered significant. These distances ($= a/\sqrt{2}$) also correspond to the As(1)–As(1) separations in the square net, and while they are long compared to a full As–As single bond length of 2.4–2.5 Å (12, 13), the possibility of weak covalent bonding between the As(1) atoms cannot be ruled out. The RE atoms are surrounded by eight As atoms in a square antiprism, at distances that reflect the diminishing size of the rare-earth on progressing from $\mathrm{LaCu}_{1.23(1)}\mathrm{As}_2$ (3.1054(5)–3.1975(5) Å) to $\mathrm{PrCu}_{1.09(1)}\mathrm{As}_2$ (3.0333(4)–3.1506(5) Å).

The presence of a square pyramidal site partially occupied by additional Cu(2) atoms is a distinguishing feature of these structures. While the five Cu(2)–As distances are nearly regular in $\mathrm{LaCu}_{1.23(1)}\mathrm{As}_2$ (2.376(3)–2.378(6)Å), the apical Cu(2)–As(2) distance is longer than the four basal Cu(2)–As(1) distances in $\mathrm{CeCu}_{1.10(1)}\mathrm{As}_2$ (2.395(10) vs 2.311(5) Å) and $\mathrm{PrCu}_{1.09(1)}\mathrm{As}_2$ (2.371(14) vs 2.306(7) Å). In $\mathrm{LaCu}_{1.23(1)}\mathrm{As}_2$, this Cu(2) site faces opposite a symmetry-equivalent site at 2.421(12) Å away. Since Cu(2)–Cu(2) bonding is unlikely to occur across an intervening As(1) layer, a pair of such facing Cu(2) atoms will experience repulsion that may account for the shortened apical Cu(2)–As(2) distance in $\mathrm{LaCu}_{1.23(1)}\mathrm{As}_2$ relative to those in $\mathrm{CeCu}_{1.10(1)}\mathrm{As}_2$ and $\mathrm{PrCu}_{1.09(1)}\mathrm{As}_2$, where the square pyramidal Cu(2) sites are staggered with respect to each other. On the other hand, the low occupancy of this site in $\mathrm{LaCu}_{1.23(1)}\mathrm{As}_2$ probably reduces the effect of this distortion,

TABLE 3
Positional and Equivalent Isotropic Thermal Parameters for $RE\mathrm{Cu}_{1+x}\mathrm{As}_2$ (RE=La, Ce, Pr)

Atom	Wyckoff position	Occupancy	x	y	z	U_{eq} (Å)[a]
			$\mathrm{LaCu}_{1.23(1)}\mathrm{As}_2$			
La	4*e*	1	0	0	0.37858(2)	0.0078(2)
Cu(1)	4*d*	1	0	$\frac{1}{2}$	$\frac{1}{4}$	0.0119(3)
Cu(2)	4*e*	0.233(8)	0	0	0.0598(3)	0.016(2)
As(1)	4*c*	1	0	$\frac{1}{2}$	0	0.0224(3)
As(2)	4*e*	1	0	0	0.17729(5)	0.0078(3)
			$\mathrm{CeCu}_{1.10(1)}\mathrm{As}_2$			
Ce	2*c*	1	$\frac{1}{4}$	$\frac{1}{4}$	0.24179(4)	0.0081(2)
Cu(1)	2*b*	1	$\frac{3}{4}$	$\frac{1}{4}$	$\frac{1}{2}$	0.0114(2)
Cu(2)	2*c*	0.101(7)	$\frac{3}{4}$	$\frac{3}{4}$	0.1127(10)	0.013(3)
As(1)	2*a*	1	$\frac{3}{4}$	$\frac{1}{4}$	0	0.0207(2)
As(2)	2*c*	1	$\frac{1}{4}$	$\frac{1}{4}$	0.64944(7)	0.0079(2)
			$\mathrm{PrCu}_{1.10(1)}\mathrm{As}_2$			
Pr	2*c*	1	$\frac{1}{4}$	$\frac{1}{4}$	0.24189(5)	0.0083(3)
Cu(1)	2*b*	1	$\frac{3}{4}$	$\frac{1}{4}$	$\frac{1}{2}$	0.0118(3)
Cu(2)	2*c*	0.09(1)	$\frac{3}{4}$	$\frac{3}{4}$	0.1134(14)	0.011(5)
As(1)	2*a*	1	$\frac{3}{4}$	$\frac{1}{4}$	0	0.0213(4)
As(2)	2*c*	1	$\frac{1}{4}$	$\frac{1}{4}$	0.6506(1)	0.0079(2)

[a] U_{eq} is defined as one-third of the trace of the orthogonalized $\mathbf{U}_{ij}$ tensor.

and certainly on a local level, two such atoms need not face each other given the $\sim \frac{1}{4}$ distribution of atoms among these sites. Whether this distribution is further ordered on the *ab* plane will be difficult to detect by X-ray diffraction. In any case, long-exposure (24 h) oscillation photographs show no evidence for superstructure along *a* or *b*.

These new $RE\mathrm{Cu}_{1+x}\mathrm{As}_2$ structures expand on the already extensive series of tetragonal structures built up by the stacking of square nets. $\mathrm{CeCu}_{1.10(1)}\mathrm{As}_2$ (or $\mathrm{PrCu}_{1.09(1)}\mathrm{As}_2$) represents a stuffed variant of the prevalent HfCuSi_2 structure type (5), which is adopted by numerous ternary pnictides such as $REM_{1-x}\mathrm{Sb}_2$ (M = Mn, Fe, Co, Cu, Zn, Ag) (4, 14, 15) and $UMPn_2$ (M = Fe, Co, Ni, Cu; Pn = P, As, Sb, Bi) (16). Similarly, $\mathrm{LaCu}_{1.23(1)}\mathrm{As}_2$ represents a stuffed variant of a parent structure type, SrZnBi_2 (17), which possesses a doubled unit cell relative to that of the HfCuSi_2 structure type. $\mathrm{LaCu}_{1.23(1)}\mathrm{As}_2$ is thus nearly isostructural to $\mathrm{CeCu}_{1.09}\mathrm{P}_{1.87}$ (18), which exhibits a pronounced deficiency in P atoms disordered over closely spaced sites within the square net. In turn, the HfCuSi_2 and SrZnBi_2 structure types are derived by inserting atoms into tetrahedral sites of the ZrSiS (19) and UGeTe (20) structure types, respectively. (We have chosen the designations "HfCuSi_2" and "SrZnBi_2" based on the most prevalent usage in the literature, but include a representative ternary copper pnictide to show more clearly the correspondence with the title compounds.) These structural relationships are illustrated as follows:

$$P4/nmm\text{:}\ \begin{matrix}\mathrm{ZrSiS}\\(\mathrm{UAs}_2)\end{matrix} \xrightarrow{\text{filling of tet. sites}} \begin{matrix}\mathrm{HfCuSi}_2\\(\mathrm{UCuAs}_2)\end{matrix}$$

$$\xrightarrow{\text{partial filling of sq. pyr. sites}} \mathrm{CeCu}_{1.10(1)}\mathrm{As}_2$$

$$I4/mmm\text{:}\ \mathrm{UGeTe} \xrightarrow{\text{filling of tet. sites}} \begin{matrix}\mathrm{SrZnBi}_2\\(\mathrm{UCuP}_2)\end{matrix}$$

$$\xrightarrow{\text{partial filling of sq. pyr. sites}} \mathrm{LaCu}_{1.23(1)}\mathrm{As}_2$$

Just as partial occupation of the tetrahedral site is common in the HfCuSi_2 structure (5, 14, 15), the nonstoichiometry of the new $RE\mathrm{Cu}_{1+x}\mathrm{As}_2$ compounds arises from partial occupation of the square pyramidal sites.

The magnetic susceptibility of $\mathrm{LaCu}_{1.23(1)}\mathrm{As}_2$ is essentially temperature-independent ($\chi_0 = -2.8 \times 10^{-4}$ emu mol^{-1}), consistent with closed-shell La^{3+} and Cu^{+} (d^{10}) species. $\mathrm{CeCu}_{1.10(1)}\mathrm{As}_2$ exhibits paramagnetic behavior down to 5 K, and the susceptibility data were fit to the Curie–Weiss law, $\chi = C/(T-\theta)$ (Fig. 2), giving the parameters $C =$ 0.601(2) emu K mol^{-1} and $\theta = -2.5(3)$ K. The small

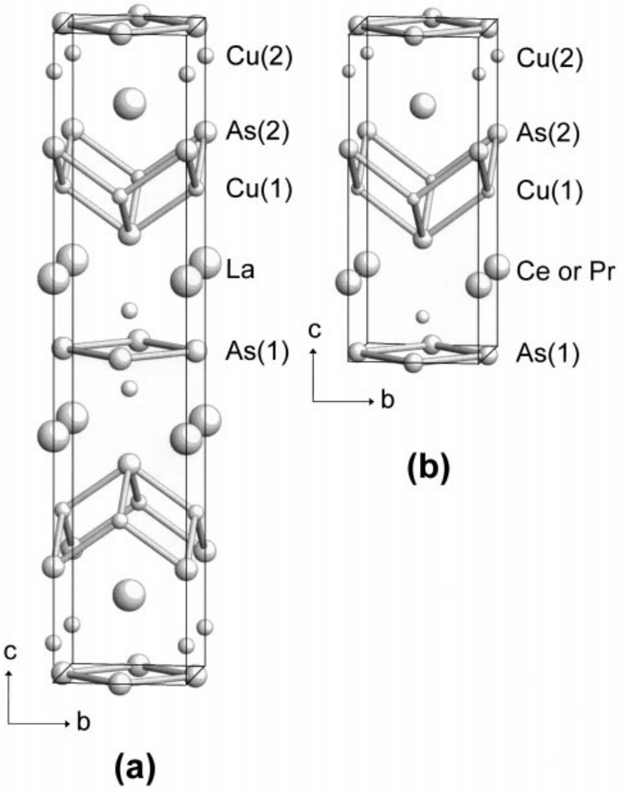

FIG. 1. View down the *a* axis of (a) $\mathrm{LaCu}_{1.23(1)}\mathrm{As}_2$ and (b) $\mathrm{CeCu}_{1.10(1)}\mathrm{As}_2$ or $\mathrm{PrCu}_{1.09(1)}\mathrm{As}_2$, with the unit cell outlined. The large circles are *RE* atoms, the small circles are Cu atoms, and the medium circles are As atoms. The Cu(2) sites are only partially occupied.

TABLE 4
Selected Interatomic Distances (Å) in $RE\mathrm{Cu}_{1+x}\mathrm{As}_2$ (RE=La, Ce, Pr)

	$\mathrm{LaCu}_{1.23(1)}\mathrm{As}_2$	$\mathrm{CeCu}_{1.10(1)}\mathrm{As}_2$	$\mathrm{PrCu}_{1.09(1)}\mathrm{As}_2$
RE–As(2) (4×)	3.1054(5)	3.0506(4)	3.0333(4)
RE–As(1) (4×)	3.1975(5)	3.1596(4)	3.1506(5)
RE–Cu(2) (4×)	3.150(2)	3.130(4)	3.115(6)
Cu(2)–As(2)	2.378(6)	2.395(10)	2.371(14)
Cu(2)–As(1) (4×)	2.376(3)	2.311(5)	2.306(7)
Cu(1)–As(2) (4×)	2.5196(6)	2.5136(5)	2.5118(6)
Cu(1)–Cu(1) (4×)	2.8921(3)	2.8472(3)	2.8345(1)
As(1)–As(1) (4×)	2.8921(3)	2.8472(3)	2.8345(1)

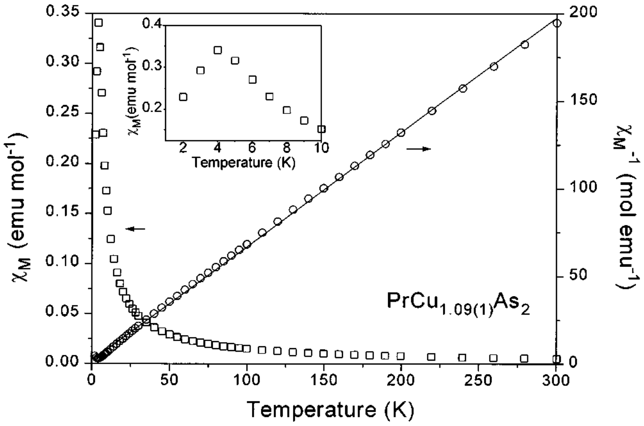

FIG. 3. Susceptibility and inverse susceptibility for $\mathrm{PrCu}_{1.09(1)}\mathrm{As}_2$ (measured at 0.1T) and fit to the Curie–Weiss law.

negative value of θ indicates a possibly weak antiferromagnetic interaction, while the effective moment of 2.19 μ_B is somewhat less than the expected value of 2.54 μ_B for Ce^{3+}. $\mathrm{PrCu}_{1.09(1)}\mathrm{As}_2$ exhibits an antiferromagnetic ordering at 4 K, and the fit of the susceptibility data to the Curie–Weiss law (Fig. 3) yields $C = 1.530(5)$ emu K mol^{-1} and $\theta = -2.6(4)$ K. The effective moment of 3.5 μ_B is consistent with the expected value of 3.58 μ_B for Pr^{3+}.

Devising a consistent bonding model for $RE\mathrm{Cu}_{1+x}\mathrm{As}_2$ is an interesting challenge. The highly electropositive *RE* atoms will form predominantly ionic bonds and adopt an oxidation state of +3, to a first approximation. The Cu–As distances are 2.31–2.52 Å, only slightly shorter than similar distances found in arsenides containing Cu(+1) (e.g., $\mathrm{SrCu_2As_2}$ 2.510(1) Å (3); $\mathrm{UCuAs_2}$, 2.514 Å (21); $\mathrm{U_2Cu_4As_5}$, 2.427(2)–2.560(3) Å (22); $\mathrm{K_3Cu_3As_2}$, 2.32 Å (23)). The ambiguity arises from the Cu(2) nonstoichiometry and the intermediate As(1)–As(1) distances (2.83–2.89 Å). If the oxidation state assignment previously proposed for $RE\mathrm{AgSb}_2$ (4) is extrapolated to an assumed isostructural, stoichiometric $RE\mathrm{CuAs}_2$ $(RE^{3+})(\mathrm{Cu}^+)(\mathrm{As(2)}^{3-})(\mathrm{As(1)}^-)$, the (−1) oxidation state for the As(1) atoms in the square net is unrealistic because the As(1)–As(1) distances are too long to be considered even as one-electron bonds. On the other hand, the assignment for $\mathrm{UCuAs_2}$, $(\mathrm{U}^{4+})(\mathrm{Cu}^+)(\mathrm{As(2)}^{3-})(\mathrm{As(1)}^{2-})$, better reflects the weakness of the As(1)–As(1) bonds (21). Assuming Cu to be in the +1 state, then, the assignment $(RE^{3+})(\mathrm{Cu}^+)_{1+x}(\mathrm{As}^{3-})(\mathrm{As}^{(1+x)-})$ is a reasonable approximation. However, the As(1)–As(1) distance is also affected by the geometrical constraints imposed by the rigidity of the tetrahedral Cu/As layer and the size of the *RE* atom, and it may not be very sensitive to changes in the As(1) oxidation state. Consequently, to maintain charge balance, either the oxidation state of some Cu atoms must change from +1 to +2 (mixed valency), or the Cu occupancy can vary, or both. Mixed valency has also been invoked to account for the *substoichiometry* observed in $\mathrm{LaCu_{0.85}Sb_2}$ (14). Since the degree of mixed valency, if any, will be small, it may be difficult to ascertain this from the magnetic data.

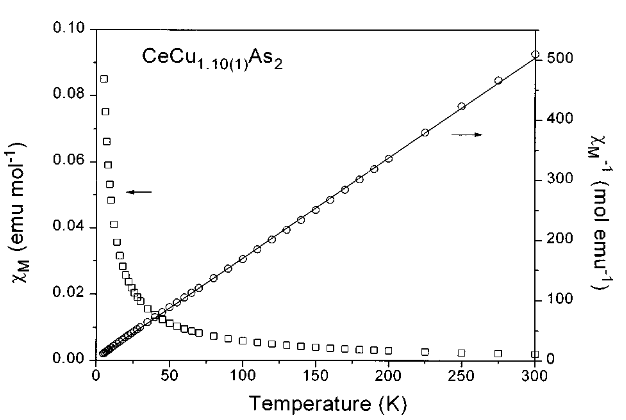

FIG. 2. Susceptibility and inverse susceptibility for $\mathrm{CeCu}_{1.10(1)}\mathrm{As}_2$ (measured at 2T) and fit of the Curie–Weiss law.

Earlier we alluded to the possibility that the partially occupied Cu site could also be modeled as a fully occupied O site, leading to a formula of "$\mathrm{LaCuAs_2O}$". While several layered pnictide oxides with closely related structures have been reported ($AE_2\mathrm{Mn}_3Pn_2\mathrm{O}_2$ (AE = Sr, Ba; Pn = P, As, Sb) (24); REMPO (M = Fe, Ru, Co) (25); $RE_3\mathrm{Cu_4P_4O_2}$ (RE = La, Ce, Nd) (26); UCuPO (27); $U_2\mathrm{Cu}_2Pn_3\mathrm{O}$ (Pn = P, As) (28); $\mathrm{ThCu}_{1-x}\mathrm{PO}$ and ThCuAsO (29)), the oxygen atoms in these structures are coordinated, *without exception*, to the electropositive metals. A hypothetical "$\mathrm{LaCuAs_2O}$" structure would have the oxygen atom coordinated to the nonmetal component (four As atoms in the square net) and would result in the chemically unlikely situation of cationic (in the square net) and anionic (in the tetrahedral Cu/As layers) arsenic species co-existing in the same structure.

On progressing from $\mathrm{LaCu}_{1.23(1)}\mathrm{As}_2$ to $\mathrm{PrCu}_{1.09(1)}\mathrm{As}_2$, not only does the Cu content decrease, but the Cu(2)–As distances in the square pyramidal site also shorten (to ∼2.3 Å), as expected upon concomitant substitution with the smaller rare-earth atoms. Since this appears to be the lower limit for realistic Cu–As bond lengths (to our knowledge, the shortest reported Cu–As distance is 2.32 Å in $K_3Cu_3As_2$ (23)), we do not anticipate the stuffed $HfCuSi_2$-type structure to extend much more beyond Pr as the rare-earth. Extrapolating to a hypothetical "$NdCu_{1+x}As_2$" using the literature cell constants for unfilled $NdCuAs_2$ (4), we calculate distances of 2.28 Å from the square pyramidal site to the neighboring As atoms, certainly too short to be reasonable.

Why $LaCu_{1.23(1)}As_2$ should adopt a doubled superstructure of $CeCu_{1.10(1)}As_2$ is not clear. Tetragonal layered structures built up from stackings of square nets are highly prone to stacking disorder or intergrowths, and many can be viewed as the superposition of slabs of more basic structures (e.g., $U_2Cu_4As_5$ (22), $U_3Ni_{3.34}P_6$ (30)). Indeed, we have evidence from powder X-ray diffraction for a disordered $LaCuAs_2$ structure built up from $HfCuSi_2$-type slabs but stacked so that the relative orientation of the tetrahedral Cu/As layers is random between adjoining unit cells along the *c* direction (31). We propose that this phenomenon may be quite common for this family of structures, the polytype formed depending on the synthetic conditions. The stability of these nonstoichiometric layered structures may depend sensitivity on temperature, and this deserves further investigation.

ACKNOWLEDGMENTS

This work was supported by the Natural Sciences and Engineering Research Council of Canada and the University of Alberta. We thank Mr. Michael Ferguson for magnetic measurements on $PrCu_{1.09(1)}As_2$ and Mr. Christopher Jones (Department of Chemistry, Cornell University) for helpful discussions.

REFERENCES

1. P. Villars, "Pearson's Handbook," Desk Ed. ASM International, Materials Park, OH, 1997.
2. A. Mewis, *Z. Naturforsch., B: Anorg. Chem., Org. Chem.* **33,** 983 (1978).
3. J. Dünner, A. Mewis, M. Roepke, and G. Michels, *Z. Anorg. Allg. Chem.* **621,** 1523 (1995).
4. M. Brylak, M. H. Möller, and W. Jeitschko, *J. Solid State Chem.* **115,** 305 (1995).
5. L. S. Andrukhiv, L. O. Lysenko, Ya. P. Yarmolyuk, and E. I. Gladyshevskii, *Dopov. Akad. Nauk Ukr. RSR, Ser. A: Fiz-Mat. Tekh. Nauki* 645 (1975).
6. "POLSQ: Program for Least-Squares Unit Cell Refinement," 1983 [modified by D. Cahen and D. Keszler, Northwestern University].
7. G. M. Sheldrick, "SHELXTL," Version 5.1. Bruker Analytical X-ray Systems, Inc., Madison, WI, 1997.
8. "International Tables for X-ray Crystallography" (Wilson, A. J. C., Ed.), Vol. C, Kluwer, Dordrecht, 1992.
9. H. Noël, Z. Zolnierek, D. Kaczorowski, and R. Troc, *J. Less-Common Met.* **132,** 327 (1987).
10. I. M. Gelato and E. Parthé, *J. Appl. Crystallogr.* **20,** 139 (1987).
11. See NAPS document No. 05530 for 8 pages of supplementary material. This is not a multi-article document. Order from NAPS c/o Microfiche Publications, P.O. Box 3513, Grand Central Station, New York, NY 10163–3513. Remit in advance in U.S. funds only $7.75 for photocopies or $5.00 for microfiche. There is a $15.00 invoicing charge on all orders filled before payment. Outside U.S. and Canada add postage of $4.50 for the first 20 pages and $1.00 for each 10 pages of material thereafter, or $1.75 for the first microfiche and $0.50 for each microfiche thereafter.
12. M. Somer, W. Carrillo-Cabrera, K. Peters, and H. G. von Schnering, *Z. Kristallogr.* **210,** 876 (1995).
13. W. Hönle, J. Lin, M. Hartweg, and H. G. von Schnering, *J. Solid State Chem.* **97,** 1 (1992).
14. G. Cordier, H. Schäfer, and P. Woll, *Z. Naturforsch., B: Anorg. Chem., Org. Chem.* **40,** 1097 (1985).
15. A. Leithe-Jasper and P. Rogl, *J. Alloys Compd.* **203,** 133 (1994).
16. D. Kaczorowski, *J. Alloys Compd.* **186,** 333 (1992).
17. G. Cordier, B. Eisenmann, and H. Schäfer, *Z. Anorg. Allg. Chem.* **426,** 205 (1976).
18. S. I. Chykhrij, G. V. Loukashouk, S. V. Oryshchyn, and Yu. B. Kuz'ma, *J. Alloys Compd.* **248,** 224 (1997).
19. A. J. Klein Haneveld and F. Jellinek, *Rec. Trav. Chim. Pays-Bas* **83,** 776 (1964).
20. A. J. Klein Haneveld and F. Jellinek, *J. Less-Common Met.* **18,** 123 (1969).
21. J. Stepien-Damm, D. Kaczorowski, and R. Troc, *J. Less-Common Met.* **132,** 15 (1987).
22. D. Kaczorowski, H. Noël, and R. Troc, *J. Less-Common Met.* **170,** 255 (1991).
23. G. Savelsberg and H. Schäfer, *Z. Naturforsch., B: Anorg. Chem., Org. Chem.* **34,** 1033 (1979).
24. S. L. Brock and S. M. Kauzlarich, *Comments Inorg. Chem.* **17,** 213 (1995).
25. B. I. Zimmer, W. Jeitschko, J. H. Albering, R. Glaum, and M. Reehuis, *J. Alloys Compd.* **229,** 238 (1995).
26. R. J. Cava, H. W. Zandbergen, J. J. Krajewski, T. Siegrist, H. Y. Hwang, and B. Batlogg, *J. Solid State Chem.* **129,** 250 (1997).
27. D. Kaczorowski, J. H. Albering, H. Noël, and W. Jeitschko, *J. Alloys Compd.* **216,** 117 (1994).
28. D. Kaczorowski, M. Potel, and H. Noël, *J. Solid State Chem.* **112,** 228 (1994).
29. J. H. Albering and W. Jeitschko, *Z. Naturforsch., B: Chem. Sci.* **51,** 257 (1996).
30. T. Ebel and W. Jeitschko, *J. Solid State Chem.* **116,** 307 (1995).
31. M. Wang and A. Mar, unpublished work.